Environmental Research 275 (2025) 121432

Contents lists available at ScienceDirect

Environmental Research

journal homepage: www.elsevier.com/locate/envres

Soil pH and total phosphorus regulate bacterial community assembly in slope restoration areas of the Tibetan Plateau's metal mining areas

Huanyu Zhou [a,b], Xiaotong Liu [a,b], Xianlei Gao [d], Yan Wang [e], Lanlan Ye [a,b], Junxi Wu [a,b,*], Mingxue Xiang [c,**]

[a] Lhasa Plateau Ecosystem Research Station, Key Laboratory of Ecosystem Network Observation and Modelling, Institute of Geographic Sciences and Natural Resources Research, Chinese Academy of Sciences, Beijing, 100101, China
[b] College of Resources and Environment, University of Chinese Academy of Sciences, Beijing, 100190, China
[c] State Key Laboratory of Plateau Ecology and Agriculture in the Three River Headwaters Region, Qinghai University, Xining, 810018, China
[d] School of Ecology and Environment, Tibet University, Lhasa, 850000, Tibet, China
[e] Lhasa Plateau Biological Research Institute, Lhasa, 850000, Tibet, China

ARTICLE INFO

Keywords:
Bacterial community diversity
Copper mining area
Nearest taxon index
Soil restoration
Tibetan plateau

ABSTRACT

Microbial community development is a crucial aspect of soil restoration. The employment of frame beams in conjunction with external soil has demonstrated efficacy in the rehabilitation of degraded roadside ecosystems within mining regions. Nonetheless, the effects of frame beams on the composition and stability of soil bacterial communities remain inadequately comprehended. We conducted a one-time soil sampling on a three-year restored slope in a large–scale metal mining area on the Tibetan Plateau, providing a snapshot of the current conditions and evaluating the restoration progress. Frame beams with external soil covers were applied at three different altitudes: A1 (4800–5000 m), A2 (4500–4700 m), and A3 (4200–4400 m). Restoration significantly altered bacterial community composition compared with controls. *Proteobacteria* had a higher relative abundance in the restoration area (average: 31.16 %), whereas *Acidobacteriota* were more abundant in the control area (average: 24.68 %). In the restoration area, soil bacterial α–diversity increased as elevation decreased, with the Shannon index rising from 5.34 (A1) to 5.82 (A3), suggesting that bacterial communities at higher altitudes are more sensitive to environmental conditions. Species turnover was the primary driving factor of β–diversity, accounting for 96.26 % under A1, 94.71 % under A2, and 91.94 % under A3, respectively. The nearest taxon index of bacterial communities shifted from negative to positive along the elevation gradient (−0.25 to 1.14), indicating an increasing trend toward community clustering. Within the bacterial co-occurrence network, soil pH and total phosphorus contribute significantly to network strength, closeness, and betweenness. Concluding, soil pH and total phosphorus were identified as key factors shaping bacterial diversity and assembly mechanisms. Our research contributes to the development of effective soil restoration strategies for alpine mining regions, providing insights into microbial community assembly and stability mechanisms.

Abbreviations:

SOC	Soil Organic Carbon	OUT	Operational Taxonomic Unit	MAT	Mean Annual Temperature
TN	Total Nitrogen	**NMDS**	Non-metric Multidimensional Scaling	**AMRH**	Annual Mean Relative Humidity
AN	Ammonium Nitrogen	**RDA**	Redundancy Analysis	**AMP**	Annual Mean Pressure
TP	Total Phosphorus	**NTI**	Nearest Taxon Index	**MAP**	Mean Annual Precipitation
AP	Available Phosphorus	**SEM**	Structural Equation Modeling	**AMWS**	Annual Mean Wind Speed

(*continued on next column*)

(*continued*)

* Corresponding author. Institute of Geographic Sciences and Natural Resources Research, Chinese Academy of Sciences (CAS), 11A, Datun Road, Chaoyang District, Beijing, 100101, China.
** Corresponding author.
E-mail addresses: wujx@igsnrr.ac.cn (J. Wu), xiangmx.20b@igsnrr.ac.cn (M. Xiang).

https://doi.org/10.1016/j.envres.2025.121432
Received 6 November 2024; Received in revised form 13 March 2025; Accepted 17 March 2025
Available online 18 March 2025

1. Introduction

The Tibetan Plateau, as one of the largest plateaus globally, exhibits a distinct continental plateau climate and is recognized as an ecologically fragile and sensitive region (Ding et al., 2013; Wu et al., 2021). Not only does it possess rich mineral resources such as copper, chromite, and lead-zinc ores, but pegmatitic deposits also contain abundant rare metals like lithium, beryllium, niobium, and tantalum (Hou et al., 2009; Qu, 2004). Mining has emerged as a major industry in the local metal production sector (Park et al., 2019). Nevertheless, mining operations and the establishment of industrial facilities often cause considerable damage to the local ecological environment (Hudson-Edwards, 2016; Santamarina et al., 2019), resulting in irreversible harm to the ecosystems (Kou et al., 2023). Due to the absence of effective environmental protection and management measures, ecological issues in mining areas have worsened over time (Gunathunga et al., 2023; Venkateswarlu et al., 2016). Significant soil erosion occurs after human-induced disturbance to soil layers in mining areas (Venkateswarlu et al., 2016). The scarcity of soil resources further exacerbates the challenge of slope ecological restoration in such areas (Gunathunga et al., 2023). Slope restoration is essential for preventing soil erosion, enhancing soil health, and improving biodiversity. It aids in restoring ecosystem functionality and mitigates the negative impacts of mining and land degradation (Li et al., 2021). Frame beam restoration is one of the prevalent methods for slope restoration, involving cement casting followed by the planting of suitable vegetation or the application of soil amendments (such as biochar or microbial agents) to stabilize surface soil (Gunathunga et al., 2023; Tang et al., 2020; Venkateswarlu et al., 2016).

Soil restoration is an exceptionally slow process (Zhang et al., 2022), involving the accumulation of soil thickness (Adriano et al., 2004), nutrient cycling (Humphrey et al., 2021), and the formation of stable pore structures within the soil. The development of microbial communities is a crucial component of the soil restoration process (Abbott et al., 2001; Adriano et al., 2004), contributing to soil health and enhancing the productivity of restored soils (Bahram et al., 2018; Beattie et al., 2018; Hou et al., 2020). Wang et al. (2024) found that restoration period is a crucial factor influencing soil microbial diversity during the slope restoration. Over a restoration period of 0–22 years, the stability of microbial communities increased with the duration of recovery. In the initial phases of slope restoration, the internal soil ecosystems remain unstable at the microscopic level (Zhang et al., 2022; García-Palacios et al., 2011) revealed that the availability of soil nutrients enhanced microbial-mediated soil functionality in three years of slope restoration. In a nine-year mining reclamation area, significant differences in microbial community structures were observed across various land use types, with soil alkaline phosphatase and total nitrogen influencing microbial community assembly (Ma et al., 2023). Microorganisms decompose organic matter, releasing nutrients that support their growth and reproduction. This process enhances microbial diversity (Xun et al., 2021) and drives soil nutrient cycles (Ling et al., 2022). Additionally, they secrete extracellular compounds that promote soil aggregation (Witzgall et al., 2021) and enhance soil physical and chemical properties, thereby improving overall soil health (Adriano et al., 2004). All these physiological and metabolic activities are also influenced by external environmental factors due to their specific geographical location, including air temperature, humidity, rainfall, and soil physicochemical properties (Kenarova et al., 2014; Song et al., 2018).

Habitat heterogeneity for microorganisms implies diverse environmental pressures (Chen et al., 2017), and variations in nutrient distribution and availability, which necessitate a range of survival strategies (Qiu et al., 2021). The composition of microbial communities experiences significant variation due to environmental stress or interspecies competition, as organisms strive to find optimal habitats within their tolerance range. This process drives species turnover and nestedness, contributing to ecosystem β–diversity (Soininen et al., 2018). This is particularly evident across varying elevation gradients in alpine mining regions, where differences in climate and soil physicochemical properties become increasingly distinct (Cui et al., 2019). Soil multifunctionality is primarily governed by a suite of edaphic parameters, notably soil pH levels, organic matter composition, and nitrogen-phosphorus stoichiometry (Liang et al., 2020; Ma et al., 2023; More and Wolkersdorfer, 2024). These biogeochemical factors collectively serve as critical drivers in shaping microbial community assembly processes through their synergistic regulation of nutrient availability and biochemical equilibrium within terrestrial ecosystems. In soils, phosphates tend to bind with minerals like calcium, iron, and aluminum, resulting in insoluble phosphates that plants cannot access (Luo et al., 2022). Consequently, phosphorus emerges as the primary limiting nutrient in terrestrial ecosystems. Vegetation succession typically diminishes biologically available phosphorus, intensifying its scarcity. Under phosphorus-deficient conditions, soil microorganisms enhance biologically available phosphorus by encoding an enzyme via the *gcd* gene, which breaks down inorganic phosphorus and mineralizes organic phosphorus (Liang et al., 2020). The starvation response genes (*phoB*, *phoR*, and *phoU*) enhance microbial phosphorus uptake, while phosphate transport genes (*pst*, *phn*, *pit*, and *Ugp*) aid in the transportation of inorganic phosphates (Alori et al., 2017). However, there remain significant research gaps concerning the dynamic patterns of phosphorus cycling facilitated by soil microorganisms in alpine mining regions. Differences in physicochemical properties contribute to variations in the distribution, species composition, and community formation processes of microbial communities across different elevation gradients (Jin et al., 2024). This raises important questions: what factors influence the variations in species composition across different habitats, and how do the diversity of microbial communities and their assembly mechanisms react to environmental changes in alpine metal mining areas (Cui et al., 2019; Green et al., 2008)?

The following research hypotheses were proposed: (1) the soil bacterial diversity and community structure vary substantially along the elevation gradient in alpine mining area; (2) in the early stages of slope restoration, soil bacterial communities exhibit an evolutionary trend from dispersion to clustering along the elevation gradient; and (3) the key drivers influencing the assemblage and stability of bacterial communities in soil may be similar between restored slopes and undisturbed areas. Overall, we studied bacterial communities in a three-year slope restoration site located in an alpine mega-metal mining region on the Tibetan Plateau. We analyzed the meteorological and soil physicochemical factors across elevation gradients that influence bacterial community diversity. Structural equation modeling was used to validate the potential mechanisms through which varying elevation environments in mining regions impact bacterial community distribution and formation.

2. Materials and methods

2.1. Study site

The study site, Qulong Copper-Polymetallic Mine (N29°38′–29°45′, E91°35′–91°46′), is located in Maizhokunggar County, Lhasa, Tibet, China (Fig. 1A). The mine is part of the Gangdese metallogenic belt with the Tethys-Himalayas (Yang et al., 2009), a globally significant porphyry copper ore metallogenic region (Hou et al., 2009). The region has a semi-dry, temperate highland climate influenced by seasonal monsoon winds. The air is typically dry, and temperatures vary sharply between daytime heat and nighttime coolness. The average annual temperature is 0.9 °C, with an average annual rainfall of 431.1 mm. The mining area is currently operational for mineral extraction, with recently established slope restoration zones (0–3 years old) strategically positioned along the

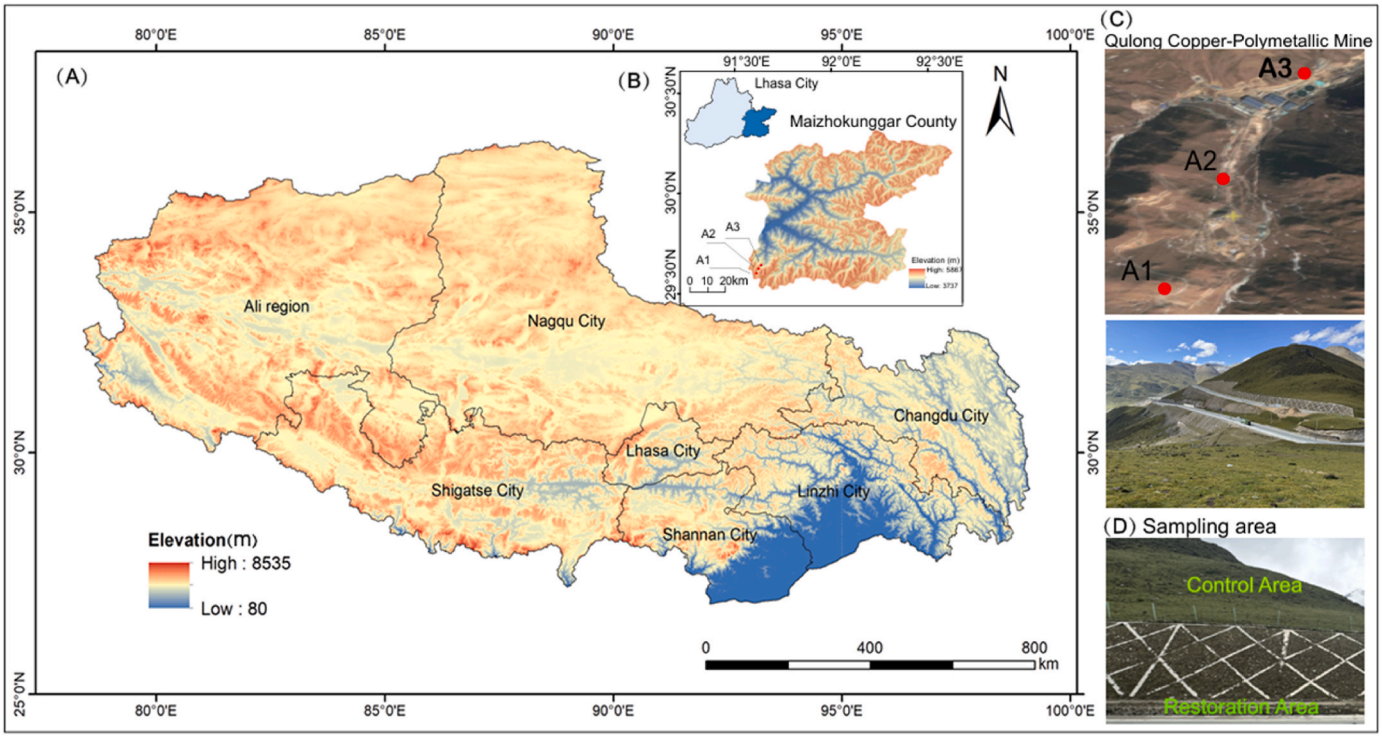

Fig. 1. Location of the Tibetan Plateau (A). Locations of the Qulong Copper-Polymetallic Mine and the study sites (A1–A3) within Maizhokunggar County, Tibet, (B). General overview of the mining area (C). Overview of each slope restoration area and the adjacent control areas (D).

mountainous access road connecting the administrative complex to the processing facilities (Fig. 1C). The soil used to fill the restoration area was derived from the topsoil of the mountain massif disrupted during mining activities. Three years after restoration, the Cu content in the high-altitude restoration area remained higher than that in the undisturbed area, whereas the Cu content in the low-altitude restoration area had decreased to levels lower than those in the undisturbed area. Given the varied timeframes and restoration methods (such as fiber spraying and bio-cell walls) in these areas, preliminary surveys indicated that the framed beam restoration method is the most effective for this mining area. In accordance with the experimental design and research objectives, areas restored for three years using the framed beam method were consistently selected across different elevation zones. According to the ecological restoration staff, each framed beam slope restoration area was stabilized by covering the steep rocky slopes with iron mesh, followed by topsoil excavated from the mining site. After the grass seeds were evenly distributed, the slopes underwent a single round of fertilization at a ratio of N:P:K = 1:1:1. No further fertilization was applied, and the slopes were regularly watered by the mining site's water truck.

2.2. Sampling

Soil samples were collected on August 10th, 2023, during the plant growing season when soil biological activity was at its peak. The sampling sites were categorized into three elevation gradients, with three corresponding meteorological stations capturing the climatic conditions at these specific elevations, and the meteorological data used in this study represent the average values from 2021 to 2023 (Table 1). Due to the discontinuity of the slope restoration areas, two slopes within each altitude gradient (with a vertical difference not exceeding 100 m) were chosen as sampling points. Concurrently, undisturbed areas of native vegetation, situated more than 100 m from the restoration areas at the same altitude gradient, were designated as the control (Fig. 1D). Both the slopes and their adjacent control areas were subjected to repeated sampling using a five-point sampling method, ensuring that each sampling point was spaced more than 5 m apart while maximizing coverage of the slope restoration area. A total of twenty sampling points were established in the restoration and control areas at each elevation zone (Table S1). Soil samples were collected from each sampling point at depths of 0–10 cm and 10–20 cm using a 5 cm diameter earth auger, with 600–700 g of fresh soil collected per sample. The samples were divided into two parts: one was sealed, labeled, and stored in a refrigerator at 2 °C for physicochemical property analysis, while the other, a composite sample from the 0–20 cm depth, was stored in liquid nitrogen below −196 °C for DNA extraction to examine microbial community assembly.

2.2.1. Soil properties and heavy metal determination

Soil for physicochemical property analysis was air-dried in a dark room and sieved through a 2 mm mesh. The soil organic carbon (SOC),

Table 1
The elevation, MAT, AMRH, AMP, MAP, and AMWS of the sample sites in different slope restoration areas, are based on data from single meteorological stations at each elevation gradient between 2021 and 2023.

Slopes	Elevation (m)	Meteorological Station Location/Elevation (m)	AMP (hPa)	MAT (°C)	AMRH (%)	MAP (mm)	AMWS (m/s)
A1	4800–5000	Phase II TSF/5060	124.8	0.6	16.3	281.3	14.9
A2	4500–4700	TBM Launching Portal/4750	140.3	1.7	14.9	443.5	9.7
A3	4200–4400	TSF/4140	345.3	3	24.1	382.6	22.7

Note: TBM is the abbreviation for Tunnel Boring Machine. The meteorological station at the A2 elevation zone is located at the TBM launching portal. TSF stands for Tailings Storage Facility, and Phase II TSF refers to the second-phase expansion of the tailings storage facility.

total nitrogen (TN), total phosphorus (TP), available nitrogen (AN), available phosphorus (AP), and copper (Cu) contents were measured. These measurements were used for correlation analysis with the bacterial community. The analyses of SOC, TN, AN, TP, AP, and Cu contents were conducted by Chengdu Baihui Testing Technology Service Co., Ltd. (Project No.: C2308131).

2.2.2. DNA extraction and high-throughput sequencing

Microbial communities were analyzed using high-throughput sequencing technology on the Illumina MiSeq platform (Caporaso et al., 2012; Cole et al., 2014). The target gene fragments were first amplified by PCR using specific primers targeting the V3-V4 region of the 16S rRNA gene. Soil for microbial property analysis was retrieved from a liquid nitrogen tank at −196 °C, and the presence of genomic DNA was confirmed using 1 % agarose gel electrophoresis. Preliminary experiments were conducted on selected samples to optimize PCR with the least number of cycles, utilizing an ABI GeneAmp® 9700. The PCR products were grouped by sample and subjected to 2 % agarose gel electrophoresis (Yeates et al., 1998). This was followed by gel excision and recovery using an AxyPrep DNA gel extraction kit (AXYGEN Scientific Inc., USA) and Tris-HCl elution. A second round of 2 % agarose gel electrophoresis was conducted to confirm detection. PCR product quantification was performed using the QuantiFluor™-ST blue fluorescence quantification system (Promega, USA). The sequenced PE reads were assembled based on overlaps, and the sequences were quality-controlled and filtered (Griffiths et al., 2000). Further analyses included sample differentiation, sequence clustering, denoising, and taxonomic classification. The final step involved high-throughput sequencing on the MiSeq platform and was conducted using the TruSeq™ DNA Sample Prep Kit.

2.3. Statistical analyses

This study used R (version 4.3.3 for Windows) to perform statistical analysis and data visualization. One-way ANOVA was selected to compare the abundance differences of bacteria at the phylum level across three elevation zones due to its robustness in testing mean differences among three or more independent groups (Quinn and Keough, 2002). However, ANOVA does not identify specific group differences; thus, Tukey's *post hoc* test (Janczyk and Pfister, 2023) was applied to control family-wise error rates while comparing all possible pairwise group contrasts. The "*vegan*" package was employed for multivariate analysis, including redundancy analysis (RDA) and non-metric multidimensional scaling (NMDS). RDA, a constrained ordination method, was chosen to explicitly model relationships between bacterial communities and environmental factors (Legendre et al., 2012), while NMDS provided a non-parametric visualization of community dissimilarities based on Bray-Curtis distances (Minchin, 1987).

For correlation analyses, the Spearman coefficient (non-parametric rank-based method) was selected over Pearson's coefficient due to its tolerance for non-normal data distributions (Hauke and Kossowski, 2011). This coefficient was integrated into Mantel tests to assess matrix correlations between environmental and microbial distance matrices, with Benjamini-Hochberg adjustment (Benjamini and Yekutieli, 2001) applied to reduce false discovery rates in multiple hypothesis testing. β–diversity decomposition was performed using the Jaccard index (Jost, 2007). Bacterial OTU abundance data from all soil samples were converted into a binary (presence/absence) format, allowing the Jaccard index to quantify community similarity and dissimilarity (1 minus similarity) among samples. This provided both an overall measure of β–diversity and pairwise β–diversity between samples. To further dissect the underlying patterns, we partitioned β–diversity into turnover and nestedness components using the '*betapart*' package (Baselga and Orme, 2012), which is well-suited for sparse microbiome datasets as it emphasizes presence-absence data. Additionally, spatial patterns of β–diversity were evaluated using multi-site dissimilarity measures. Network topological parameters (node Strength, Closeness, Betweenness) were calculated via the "*igraph*" package, which specializes in graph theory metrics (Ju et al., 2016), while Cytoscape (version 3.10.2 for Windows) was chosen for visualization due to its interactive network layout customization capabilities (Shannon et al., 2003). The calculation of node Strength, Closeness, and Betweenness in the co-occurrence network are presented in Table S3. MEGA (version 11.0.13 for Windows) was employed to construct co-phylogenetic trees of bacterial communities from different sample sites (Tamura et al., 2021), while the microbial nearest taxon index was calculated using the "*NST*" package.

PICRUSt2 (Douglas et al., 2020) was implemented for functional prediction, leveraging the phylogenetic placement of 16S rRNA sequences against reference databases (SILVA) to infer KEGG pathways (Kanehisa and Goto, 2000). The results were normalized to obtain predicted KEGG pathway abundance information. Principal coordinates analysis (PCoA) was performed on meteorological factors using the "*ape*" package, where temperature, relative humidity, and pressure data were dimension-reduced, with the first PCoA axis being used as the "Climate Factors" data. While this approach is computationally efficient, potential limitations include dependency on reference database completeness. Structural equation modeling (SEM) via the "*piecewiseSEM*" package was adopted to evaluate causal pathways among meteorological, soil, and microbial variables. SEM is advantageous for partitioning direct and indirect effects in complex systems but requires careful model specification to avoid overfitting (Lefcheck, 2016). All visualization workflows were standardized using the "*ggplot2*" package for its reproducible grammar-of-graphics framework (Wickham, 2016).

3. Results

3.1. Bacterial community composition and diversity

Bacterial communities were observed across different elevation gradients in the mining area restoration and control sites revealing a distribution of sequences across 481 genera, 309 families, and 38 phyla. The top ten most abundant phyla are presented in Table 2, including *Proteobacteria*, *Chloroflexi*, *Acidobacteriota*, *Actinobacteriota*, *Patescibacteria*, and *Bacteroidota*. These six phyla constituted over 80 % of all sequences in the soil samples. Additionally, *Gemmatimonadota*, *Verrucomicrobiota*, *Methylomirabilota*, and *Firmicutes* were identified, with the remaining less abundant phyla categorized as "others", accounting for 2.50 %–5.65 % of the total abundance.

Proteobacteria were found to be the most abundant in the restoration areas: A1R (25.16 %); A2R (33.44 %); A3R (34.89 %). Meanwhile, *Acidobacteriota* exhibited the highest proportions in the control area. The distribution of various bacterial taxa across different altitude gradients revealed distinct patterns. In the restoration areas, *Proteobacteria*, *Actinobacteriota*, and *Acidobacteriota* significantly increased with altitude. In

Table 2
The average relative abundance of the top ten most abundant bacterial and other phyla in the restoration and control areas across three elevation gradients.

Study sites						
Phylum	A1R (%)	A1CK (%)	A2R (%)	A2CK (%)	A3R (%)	A3CK (%)
Proteobacteria	25.16	25.28	33.44	21.58	34.89	19.73
Actinobacteriota	14.49	12.53	17.74	12.54	18.69	12.97
Acidobacteriota	17.96	22.76	14.24	21.22	19.19	30.05
Chloroflexi	19.07	17.15	11.00	16.98	9.87	14.35
Patescibacteria	6.35	3.60	6.34	6.54	1.77	3.97
Bacteroidota	4.69	1.31	7.47	4.12	8.44	1.71
Gemmatimonadota	4.55	2.06	4.28	2.29	3.55	3.07
Verrucomicrobiota	1.72	3.89	1.42	3.67	0.95	4.59
Methylomirabilota	1.50	3.16	0.27	1.54	0.06	4.09
Firmicutes	0.24	3.57	0.35	3.88	0.17	1.19
Others	4.27	4.69	3.45	5.65	2.51	4.28

contrast, in the control area, the abundances of *Acidobacteriota* and *Gemmatimonadota* increased as altitude decreased ($p < 0.01$).

In restoration areas, A2R and A3R exhibited higher bacterial α–diversity compared to A1R (Table 3). The Shannon index and ACE index (Fig. 2A and B) showed a significant increase from A1R to A2R and A3R. Notably, when comparing the difference in bacterial diversity between the control and restoration areas at different elevations, the difference at A1 (i.e., A1CK–A1R) was significantly higher than those at A2 and A3. The findings from NMDS suggested that the gradient may drive the differentiation among the samples. The bacterial communities in the restoration areas (Fig. 2C) exhibited a distinct separation (stress <0.1). In the control (Fig. 2D), differences in bacterial species composition among different elevation samples were insignificant.

3.2. Decomposition of bacterial β–diversity

The variations in bacterial composition within the mining area were predominantly driven by species turnover (Table 4). The proportion of shared bacterial species between the restoration and control areas increases along the elevational gradient. The contribution of turnover to β–diversity decreased with the decreasing altitude ($p < 0.05$), accounting for 96.26 %, 94.71 %, and 91.94 % in the A1R, A2R, and A3R zones respectively. No significant differences were observed in the variation of β−diversity components across elevation bands in the control area.

The ternary plot visualized the similarity, turnover, and nestedness components between sample pairs in each study area (Fig. 3). The mean values indicated that in the restoration area, similarity increased, turnover decreased, and overall data density rose as elevation decreased. In the control area, similarity initially decreased and then increased, while turnover and data density first increased and then declined with decreasing elevation. The similarity of values between A1 and A3 suggested that sampling points at the A2 elevation band were less stable.

3.3. Mantel test of bacteria and soil properties

In restoration areas, the dominant factors influencing microbial communities across various altitudes were soil nitrogen and pH levels in both surface and subsurface layers (Fig. 4A, $p < 0.01$). Phosphorus and SOC primarily impacted the A2R and A3R zones. Among the climatic factors, temperature and pressure significantly affected bacterial communities across all elevation zones, while humidity played a crucial role in the A3R zone ($p < 0.01$).

3.4. RDA analysis of bacteria and soil properties

Redundancy analysis (RDA) for bacterial communities and soil environmental factors revealed a similar explanatory power across both soil layers. The first two axes of the RDA accounted for 58.58 %, 55.20 %, and 60.49 % of the variation in bacterial community composition in the surface soil layer of the A1, A2, and A3 zones, respectively (Fig. 5A–C), and 57.26 %, 51.48 %, and 61.50 % in the subsurface soil layer, respectively (Fig. 5D–F). Soil parameters exhibited varying degrees of explanatory power for bacterial community variation. Soil pH consistently showed a significant positive correlation with changes in bacterial community variation structure and diversity in the restoration area, with exceptionally high explanatory power in the A1 and A2 elevation zones ($r^2 = 0.88$–0.92), which slightly decreased in A3. Highly correlated parameters (SOC, TN, and AN) exerted a persistent and strong influence on bacterial communities in the control area. Their explanatory power increased along the elevation gradient and is more pronounced in subsurface soil layers than in surface layers. TP and AP influenced both the restoration and control areas in the A1 and A2 elevation zones, with most bacterial community variations being positively correlated with them. Notably, TP in A1 exhibited an explanatory power of 0.49, second only to pH. At lower elevations (A3), both surface and subsurface soil TP and AP demonstrated high explanatory power, with TP playing a dominant role in shaping bacterial communities in the control area, while AP has a stronger impact on the restoration area.

3.5. Co-occurrence networks between bacteria and soil properties at the phylum level

The co-occurrence networks of bacteria in the restoration areas (Fig. 6A) indicated that the networks of soil physicochemical factors and bacterial communities became simpler and more independent as altitude decreased. In the A1R zone, a sensitive ecosystem area, soil pH, TP, and AP in both surface and subsurface layers collectively influenced a microbial network comprising 106 OTUs. In contrast, the microbial network influenced by SOC, TN, and AN consists of 83 OTUs. In the A2R zone, the network influenced by pH and nitrogen comprises 118 OTUs, while the network governed by TP and AP consists of 67 OTUs. In the A3R zone, the network is smaller but more specific; soil pH in both surface and subsurface layers independently influenced a network of 79 OTUs, while TP and Cu together affected a network of 67 OTUs, and AP governed a network of 44 OTUs. Cu was predominated in the A1CK and A2CK zones. However, its influence weakened in A3CK, where SOC, TP, AN, and TN jointly affected a larger network of 109 OTUs. Although the roles of pH and TP were diminished by Cu, they still independently affected portions of the co-occurrence networks across different elevation zones.

The contribution of each soil parameter as a node to network stability in the co-occurrence network is fully presented in Table S4. The node strength of each soil property within the restoration area was notably high (Fig. 6B), with the strength in the A1R and A2R zones exceeding that in the A3R. In both the restoration and control areas, the TP and AP exhibited the highest centrality, while the pH, TP, and AP demonstrated higher betweenness, thereby contributing to network stability as “bridge” nodes. The contributions of SOC, TN, and AN to network stability were primarily reflected in their correlation-dominated strength, while soil pH, TP, and AP made significant contributions to all three stability indicators, with TP, particularly in the subsurface soil, showing especially strong contributions in both the restoration and control areas.

3.6. The relationship between bacterial community properties and environmental variation

In the phylogenetic assembly of soil bacterial communities,

Table 3
The microbial diversity index and the community assembly index across different study sites.

Sample sites	Shannon index	ACE index	NMDS1	MMDS2	NTI
A1R	5.34 ± 0.25^{b}	2245.66 ± 285.96^{b}	-0.28 ± 0.26^{d}	-0.05 ± 0.04^{a}	-0.25 ± 1.28^{b}
A1CK	5.69 ± 0.33^{ab}	3011.98 ± 389.43^{a}	0.14 ± 0.11^{ab}	-0.03 ± 0.11^{a}	0.48 ± 0.79^{ab}
A2R	5.91 ± 0.41^{a}	2733.10 ± 386.66^{ab}	0.02 ± 0.11^{bc}	0.08 ± 0.18^{a}	0.82 ± 0.47^{ab}
A2CK	5.53 ± 0.31^{ab}	2570.24 ± 558.23^{ab}	-0.14 ± 0.28^{cd}	0.02 ± 0.20^{a}	-0.35 ± 1.06^{b}
A3R	5.82 ± 0.27^{a}	2823.97 ± 351.85^{a}	0.26 ± 0.05^{a}	-0.03 ± 0.05^{a}	1.14 ± 0.64^{a}
A3CK	5.59 ± 0.22^{ab}	2749.09 ± 345.11^{ab}	0 ± 0.15^{bc}	0 ± 0.13^{a}	1.12 ± 0.76^{a}

Note: The values of NMDS1 and NMDS2 represent the mean positions of sample species along the horizontal and vertical axes of the NMDS plot, respectively. Different letters indicate significant differences amongst the six survey regions (Tukey’s test, $p < 0.05$).

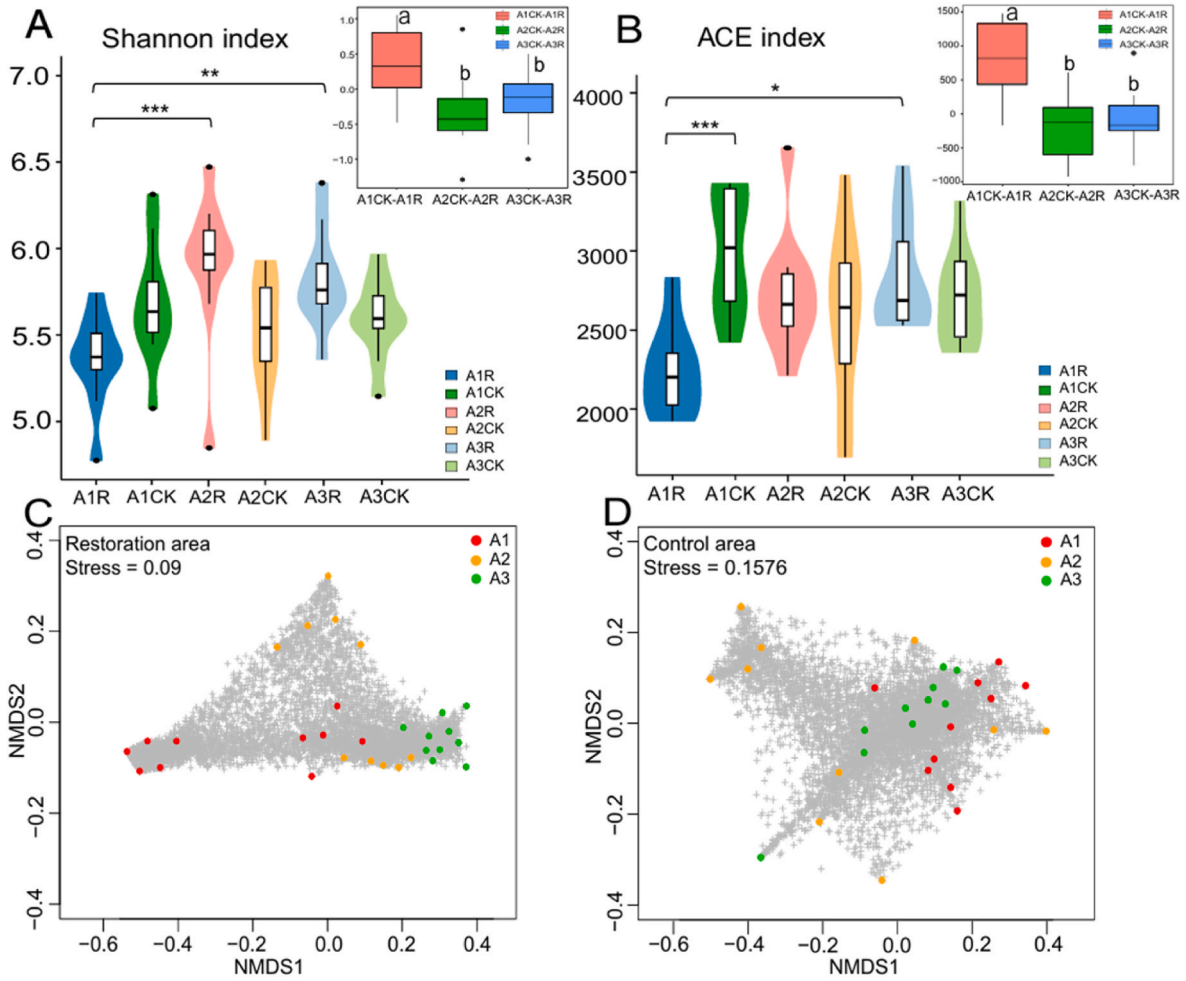

Fig. 2. Bacterial diversity between different altitudes and study areas: Shannon index (A), ACE index (B). The illustration in the upper right shows the difference between the control area and the restored area across three elevation gradients. NMDS based on both species and sample sites, reveals the bacterial β–diversity in the mining area: restoration area (C), and control area (D). Different colors represent sample sites from different elevations. Asterisks denote the significance level ("*", $p < 0.05$; "**", $p < 0.01$; "***", $p < 0.001$). Different letters indicate significant differences (Tukey's test, $p < 0.05$). (For interpretation of the references to color in this figure legend, the reader is referred to the Web version of this article.)

Table 4
The similarity, turnover, and nestedness components of bacterial communities across study sites, and the proportional contributions of turnover and nestedness to β−diversity.

Sampling sites	Similarity	Total Beta Diversity		Contribution of Turnover (%)	Contribution of Nestedness (%)
		Turnover	Nestedness		
A1R	0.159	0.810	0.031	96.26^{a}	3.74^{C}
A1CK	0.176	0.793	0.031	96.27^{ab}	3.73^{BC}
A2R	0.152	0.803	0.045	94.71^{b}	5.29^{B}
A2CK	0.150	0.826	0.024	97.22^{a}	2.78^{C}
A3R	0.246	0.693	0.061	91.94^{c}	8.06^{A}
A3CK	0.184	0.785	0.031	96.24^{ab}	3.76^{BC}

Note: Lowercase letters indicate significant differences in the contribution of Turnover to β−diversity among study areas, while uppercase letters indicate significant differences in the contribution of Nestedness (Tukey's test, $p < 0.05$).

subsurface soil pH and TP in the mining area not only impacted the diversity of bacterial communities but also influenced their community assembly mechanisms, shifting from dispersal to clustering development. The structural equation model (Fig. 7) showed that climate factors such as air temperature, humidity, and pressure, affected soil nutrient availability, and jointly influenced the characteristics of bacterial communities. In restoration areas, climate factors, soil pH, and TP had a positive correlation with the NTI index of the bacterial community, exhibiting a total effect of 0.523, 0.442, and 0.759, respectively (Fig. 7D). Climate factors and pH negatively affected the turnover component of bacterial community β–diversity, whereas TP exhibited a positive effect, with a total effect of −0.810, −0.252, and 0.374, respectively (Fig. 7C). Both climate factors and TP negatively influenced the α–diversity of bacterial communities, with a total effect of −0.176 and −0.849 (Fig. 7B). The model was also applicable in the control areas, however, in contrast to the restoration areas, the effect of TP on the turnover component of bacterial community β–diversity shifted from positive to negative, with a total effect of −0.498 (Fig. 7G). Moreover,

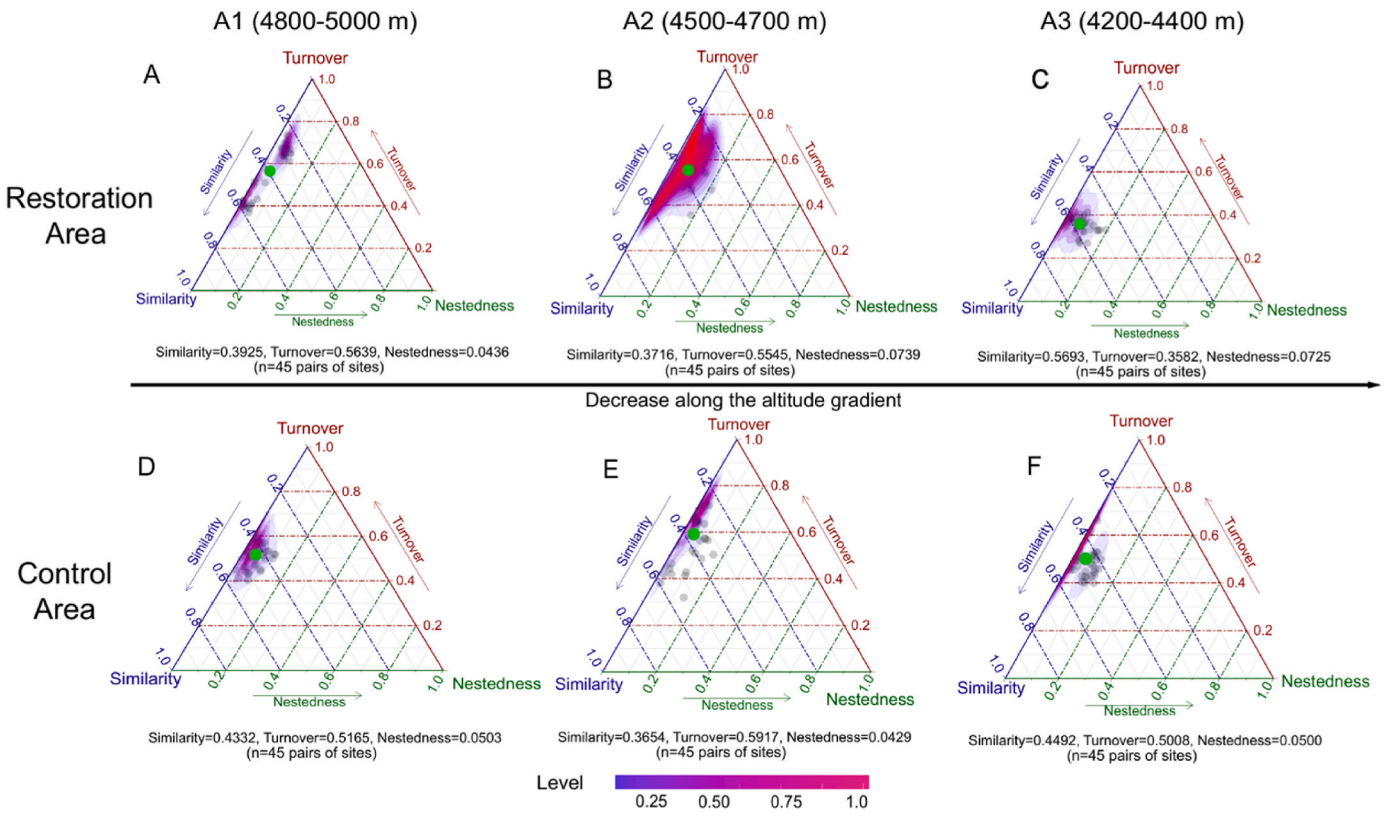

Fig. 3. Ternary plots were used to compare the bacterial β–diversity composition between restoration areas and the control areas across different elevations in the mining region: restoration areas (A–C), and control areas (D–F). The horizontal axis signifies the proportion of nestedness, whereas the upper-left and upper-right axes respectively denote the proportions of similarity and turnover. Each point on the plot corresponds to a pair of samples, the location was determined by the values of the similarity, turnover, and nestedness matrices, with each triplet summing to one. The green dot illustrates the average point of all data within the ternary plot, with its specific values provided beneath the figure. The lever serves to visually represent the data density in the ternary plot via variations in color and transparency. (For interpretation of the references to color in this figure legend, the reader is referred to the Web version of this article.)

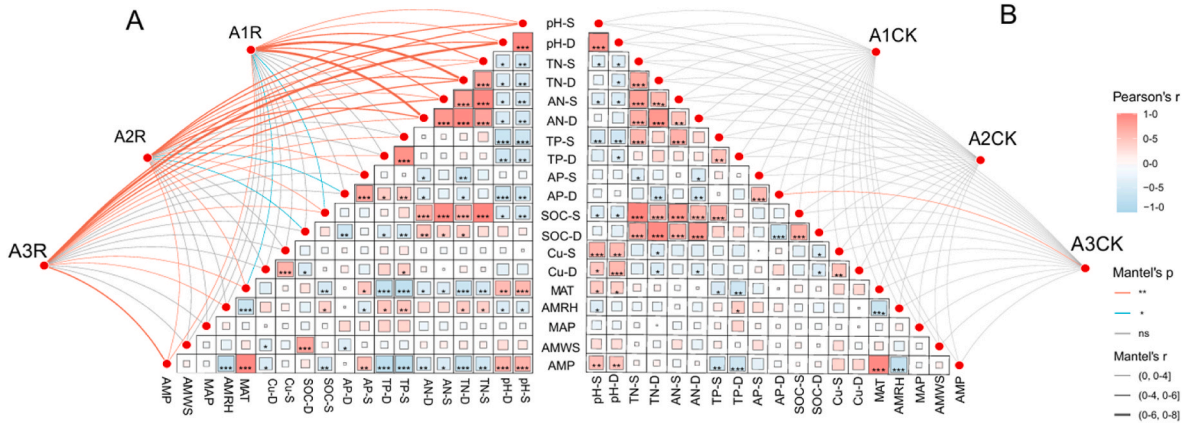

Fig. 4. Analysis of the correlations between the bacterial communities and physicochemical properties of soil across different elevations in both the restoration area (A) and control area (B). The Pairwise comparisons of the analyzed factors were presented with a color gradient denoting Spearman's correlation coefficient. Mantel's *r* indicates the strength of the correlation between factors. Mantel's *p* indicates whether the correlation is significant. (For interpretation of the references to color in this figure legend, the reader is referred to the Web version of this article.)

the impact of climate factors on bacterial community α–diversity transitioned from negative to positive, with a total effect of 0.533 (Fig. 7F).

4. Discussion

4.1. Differences in bacterial community composition and diversity across various elevation zones within the mining area

The observed differences in bacterial species composition between the restoration and the control areas highlight the functional roles of various microbial groups during soil recovery. This suggests that specific

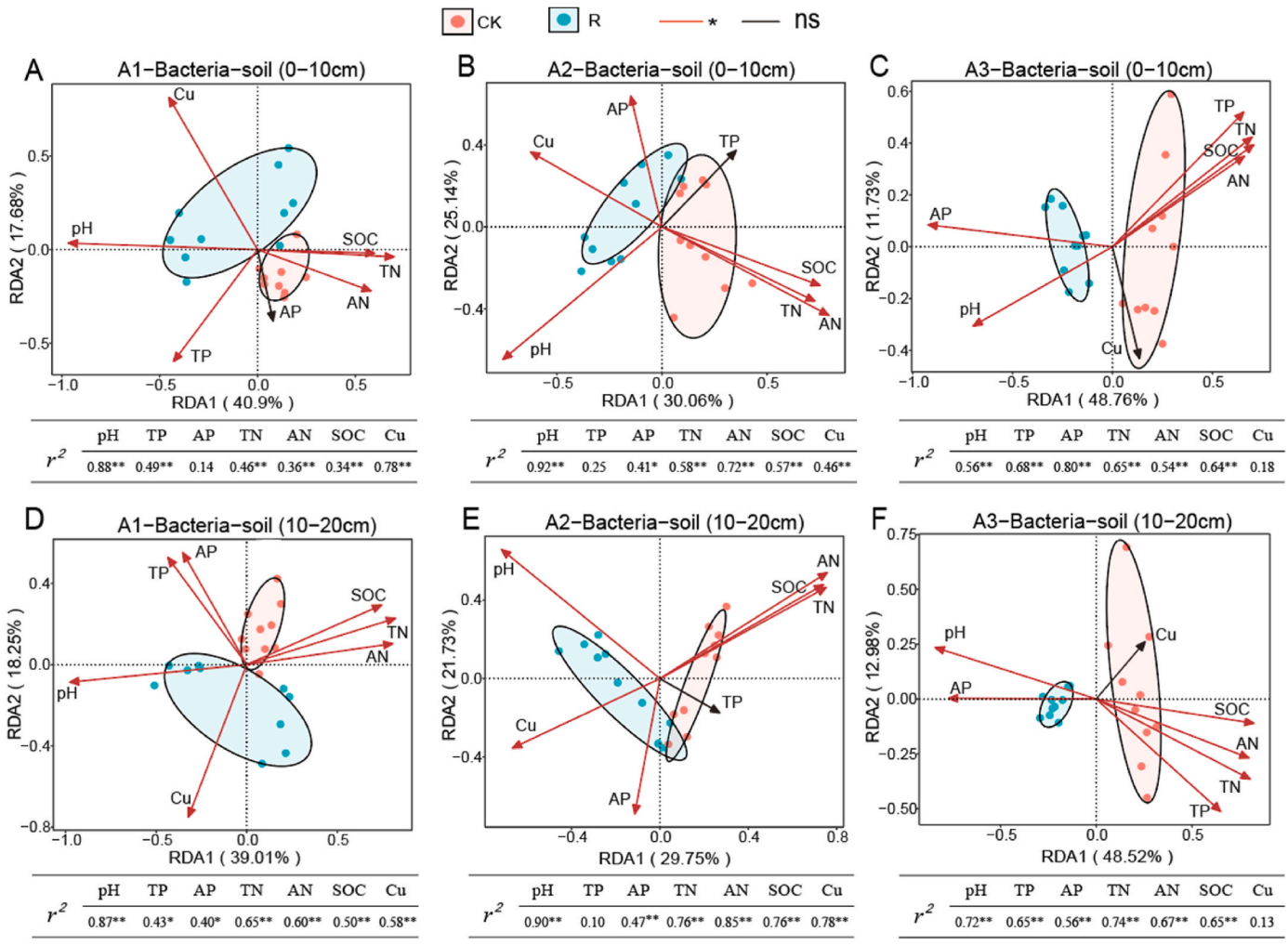

	pH	TP	AP	TN	AN	SOC	Cu
r^2	0.88**	0.49**	0.14	0.46**	0.36**	0.34**	0.78**

	pH	TP	AP	TN	AN	SOC	Cu
r^2	0.92**	0.25	0.41*	0.58**	0.72**	0.57**	0.46**

	pH	TP	AP	TN	AN	SOC	Cu
r^2	0.56**	0.68**	0.80**	0.65**	0.54**	0.64**	0.18

	pH	TP	AP	TN	AN	SOC	Cu
r^2	0.87**	0.43*	0.40*	0.65**	0.60**	0.50**	0.58**

	pH	TP	AP	TN	AN	SOC	Cu
r^2	0.90**	0.10	0.47**	0.76**	0.85**	0.76**	0.78**

	pH	TP	AP	TN	AN	SOC	Cu
r^2	0.72**	0.65**	0.56**	0.74**	0.67**	0.65**	0.13

Fig. 5. The RDA of bacterial OTU tables and soil environmental factors, DCA analyze: Axis lengths ≤3. The 0–10 cm soil layer (A–C) and the 10–20 cm soil layer (D–F). Different colors are used to distinguish samples from restoration areas and control areas. Significant effects are denoted by red arrows, where the length of the arrow represents the strength of the influence. The angle between the direction of the arrow and the coordinate axis signifies both the positive or negative nature and magnitude of the correlation. The vertical distance from the sample point to the arrow indicates the intensity of the environmental factor's influence on that specific sample point. The proportion of Variance Explained (r^2) by soil parameters for bacterial community variation in RDA, determined by permutation tests, and their statistical significance. Asterisks denote the significance level: "*", $p < 0.05$; "**", $p < 0.01$; "***", $p < 0.001$. (For interpretation of the references to color in this figure legend, the reader is referred to the Web version of this article.)

microbial groups may be particularly beneficial for soil restoration (Ling et al., 2022; Wang et al., 2024). These findings are consistent with the study by Zuo et al. (2023) on microorganisms in the tailings soil of lead-zinc mines in karst regions and by Wang et al. (2024) on roadside slope restoration. Our research indicates that *Proteobacteria* and *Actinobacteriota* are more prevalent in the restoration area (Table 2), playing a pivotal role in soil cycling and improving soil structure (Lu et al., 2024). *Proteobacteria* contribute to nutrient cycling by decomposing organic matter, promoting soil aggregate formation, and improving soil structure (Ling et al., 2022; Wang et al., 2023), which is especially crucial for soil ecosystems in the early stages of recovery. The presence of heavy metals in the soil also influences the bacterial community structure (Zuo et al., 2023). The Cu content in both the surface and subsurface soils of the A1R and A2R zones is higher than that in the control areas (Table S2). *Actinobacteriota* has multiple genes encoding heavy metal oxidases and exhibits strong tolerance to heavy metals, thereby reducing the bioavailability of heavy metal content in the soil (Altimira et al., 2012; Bohan et al., 2022; Zhang et al., 2024). The soil pH in the control area is acidic, which likely contributes to the higher proportion of acidophilic bacteria, specifically *Acidobacteriota*. These bacteria not only decompose various organic residues but also exhibit high sensitivity to environmental changes, thereby indicating the overall functionality and stability of the soil ecosystem (Kou et al., 2023).

Diversity indices were frequently employed to gauge the stability of microbial communities (Xun et al., 2021), and they serve as a measure of soil ecosystem multifunctionality (Bastida et al., 2021; Wagg et al., 2014; Wu et al., 2022). Prior research has demonstrated marked variations in soil microbial composition across distinct successional stages (Jiang et al., 2021). From the perspective of environmental gradients, bacterial α–diversity increases from higher to lower altitudes (Fig. 2A and B). Both indices indicate that in the A1 zone, the α–diversity of the control area is significantly greater than that of the restoration area. However, this trend is absent in the A2 and A3 zones. Banerjee et al. (2024) discovered that microbial α–diversity diminished in the contaminated soils of mining areas subjected to PHEs pollution and alkalinity stress, implying that higher altitude slopes present greater restoration challenges (Li et al., 2022). Environmental factors, such as nutrients or pollutants, contribute to the dispersed distribution of bacterial communities in the restoration area along the altitudinal gradient (Song et al., 2018). Particularly in the A1 zone, where community separation is pronounced along the NMDS axes (Fig. 2C and D). The negative NTI index (Table 3) observed in the A1R zone signifies

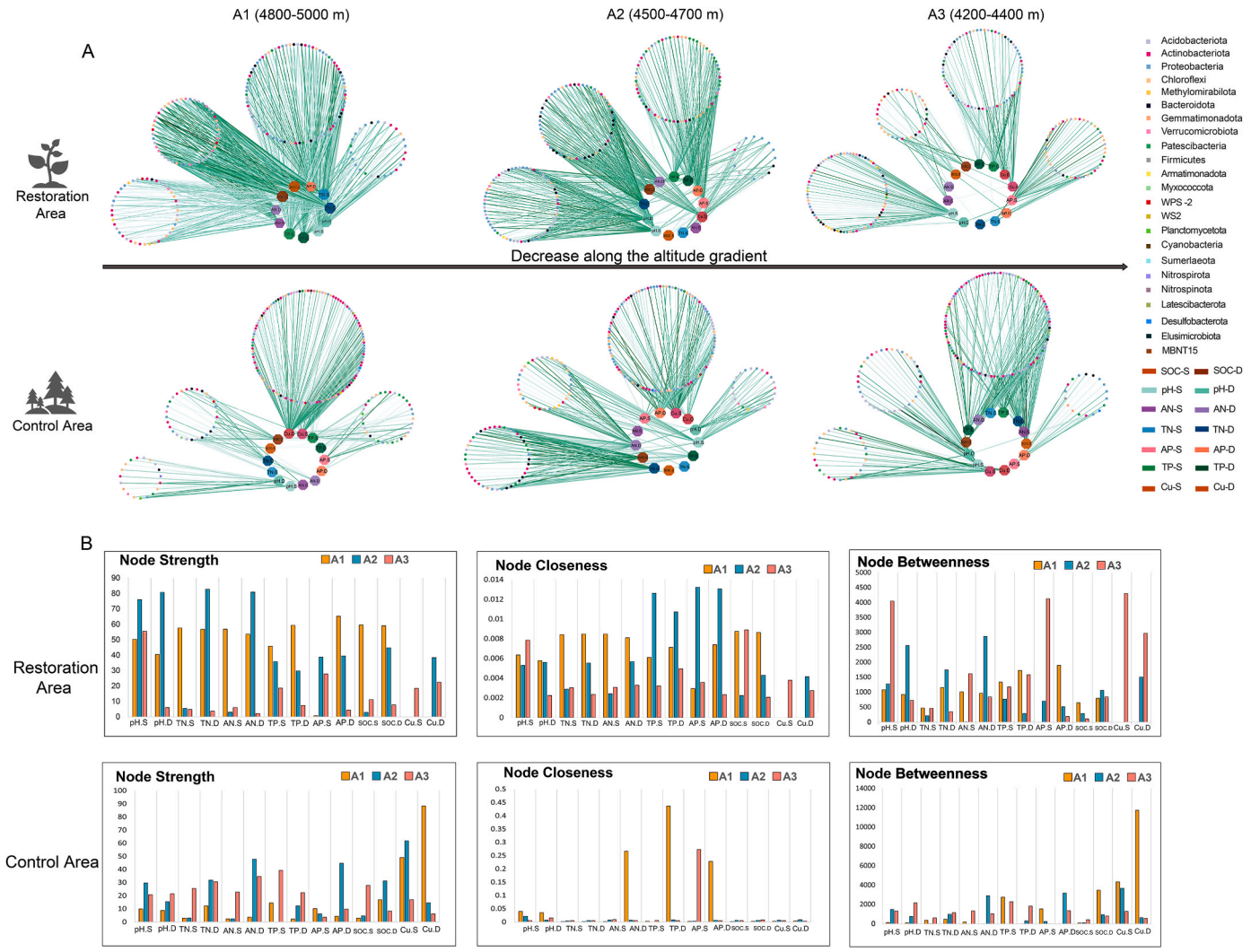

Fig. 6. The microbial co-occurrence network constructed between bacteria and environmental factors (A). To regulate the size and precision of these networks, OTU units within each sample were filtered based on their abundance values (abundance >0.005 in the restoration area and >0.001 in the control area). The distance matrix between each OTU unit and environmental factor was calculated using the Spearman coefficient. We further refined our selection by choosing relationships with a correlation coefficient exceeding 0.7 and a significance level below 0.05 to construct the network's edge list. These OTU units were annotated at the phylum level, and the microbial network was constructed and visualized using Cytoscape, wherein line thickness signifies weight. Node strength, closeness, and betweenness corresponding to various environmental factors are presented (B).

overdispersion, implying that the development and assembly of bacterial communities occur at a slower rate at higher altitudes compared to lower ones.

Spatial turnover refers to the replacement of certain species by others due to environmental, spatial, and historical constraints (Baselga, 2010). In the decomposition of bacterial community β–diversity (Fig. 3), we also verified that species turnover is the primary force driving differences in bacterial community composition (Jost, 2007). Disturbances engendered by mining activities led to the segregation of bacterial communities, thereby augmenting β–diversity which in turn facilitated the adaptation of these communities to their respective habitats (Xu et al., 2020). During soil restoration, new dominant species continuously replace the original populations (Soininen et al., 2018). Furthermore, the contribution rate of turnover to β–diversity decreases along the altitudinal gradient, indicating that as altitude decreases, the environmental stress on microbial communities is mitigated. Notably, after fully accounting for β–diversity driven by richness differences and species spatial variation (Baselga, 2012), we observed a declining trend in the contribution of turnover to β–diversity along the elevation gradient in the restoration area (from 96.26 % to 91.94 %). Meanwhile, the similarity component among samples in each study area increased steadily (from 0.159 to 0.246), along with a rise in data density driven by similarity. These findings suggest that species replacement within bacterial communities may be reduced at lower elevations in the restoration area, allowing more dominant clusters to persist. Compared to bacterial communities in high-elevation restoration areas, those at lower elevations are likely subjected to lower environmental pressures.

4.2. *Response of bacterial community structure to environmental physicochemical characteristics during soil restoration*

Microbial community composition exhibits sensitivity to environmental alterations and can swiftly adapt to them. The primary drivers of bacterial community dissimilarity may be the soil's physicochemical properties and climatic factors across altitudinal gradients (Kuang et al., 2016; Pérez Castro et al., 2019). The Mantel test (Fig. 4) indicates a strong correlation between the development and stabilization of soil ecosystems and the interactions between microbes and physicochemical properties (Li et al., 2024). Soil pH, carbon, nitrogen, and phosphorus are intimately associated with microorganisms (Gunathunga et al.,

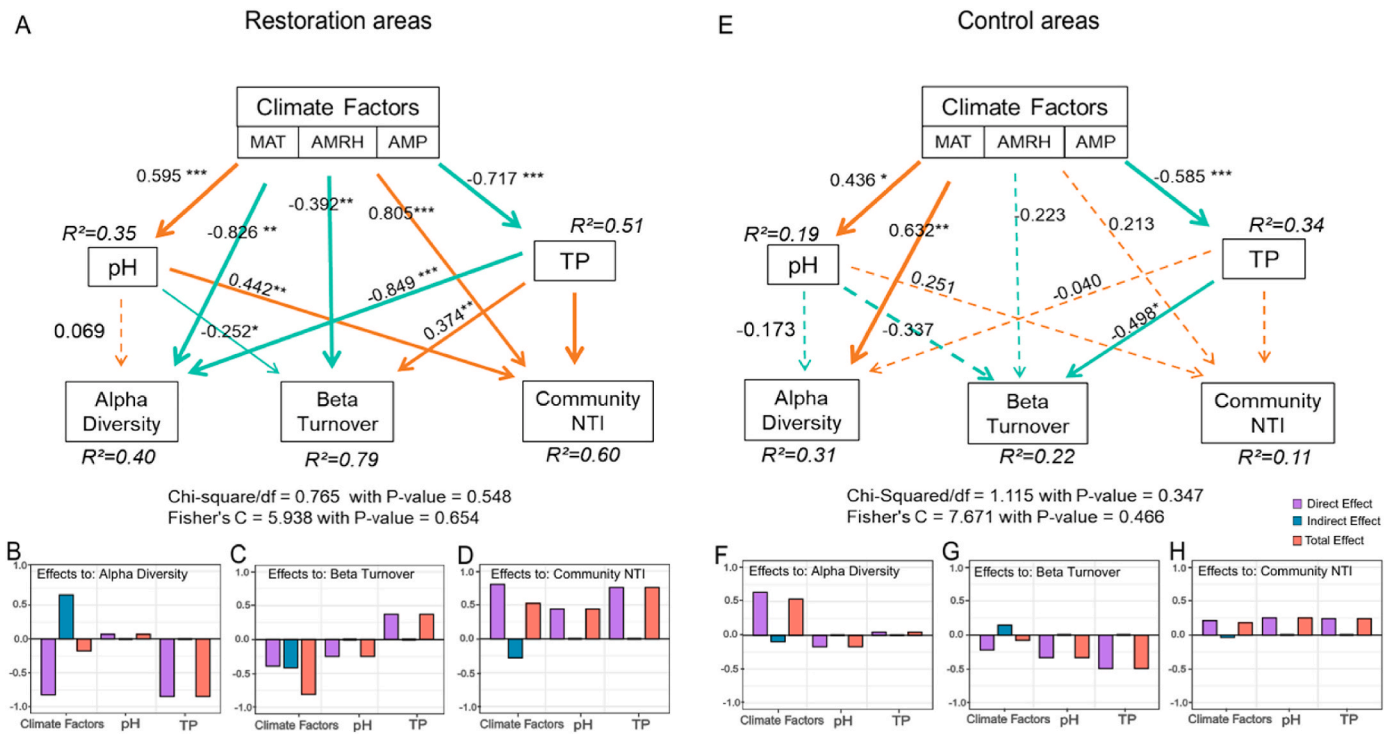

Fig. 7. The SEM models for restoration areas (A) and control areas (E). Solid arrows denote significant effects, while dashed arrows indicate non-significant effects. B–D and F–H respectively represent the direct, indirect, and total effects of predictor factors on various predicted indicators. The Chi-square/df ratio represents the quotient of the chi-square value and the degrees of freedom; Fisher's C-statistic and the corresponding p-value are also provided.

2023). Microorganisms efficiently utilize available organic matter in their environment, including humus, plant residues, and cellulose, to generate increased biomass (Wagg et al., 2014). During this process, microorganisms decompose soil organic nitrogen to produce ammonia nitrogen, thereby synthesizing the necessary biomass nitrogen for their growth. This not only influences the structure of the microbial community but also directly impacts the processes of soil carbon and nitrogen mineralization, as well as the C:N ratio (Tian et al., 2024; Zhang et al., 2022). This effect persists even as the entire soil ecosystem evolves towards a stable state (CK).

Our study refines and amplifies the influence of various soil factors on bacterial community structure (Fig. 5). We found that soil pH exerts a significant impact on bacterial community variation across different elevation gradients. Soil pH is a significant predictor of microbial community structure in tailings, as bacterial survival and function typically operate within a narrow optimal pH range (Chen et al., 2013). pH is a crucial environmental parameter during the soil recovery process, directly influencing a series of physiological and metabolic activities in the soil (Atasoy and Cetecioglu, 2022; More and Wolkersdorfer, 2024), such as enzyme catalysis (Tang et al., 2020) and fatty acid synthesis (Atasoy et al., 2019; Bevilacqua et al., 2021). Liu et al. (2023) found that differences in soil pH between mining areas and surrounding regions led to significant variations in bacterial relative abundance, diversity, and community structure. This aligns with our research findings, where at higher altitudes (A1), pH has a more pronounced influence and exhibits a stronger correlation with microbial community structure (Fig. 4A and Fig. S1). At higher elevation zones (A1, A2), permutation tests revealed that pH accounted for 87 %–92 % of the variation in bacterial community composition (Fig. 5). However, the influence of carbon and nitrogen on bacterial communities is more pronounced in high-altitude areas with slower restoration progress (A1R) during the early stages of soil recovery, while phosphorus exerts a sustained influence on the overall soil restoration process (Luo et al., 2022). In RDA analysis, TP and AP influence bacterial communities in both the restoration and control areas. At the A3 elevation zone, TP explains 68 % (r^2 = 0.68) of the variation in surface soil bacterial communities, while AP accounts for 80 % (r^2 = 0.80).

Complex organic processes in the soil often lead to the formation of organic phosphorus products resistant to decomposition. Research has demonstrated that following the ecological restoration of mining-degraded land, the phosphorus cycle in the soil is enhanced (Gao et al., 2024; Li et al., 2024; Wang et al., 2023). This is because the microbial *gcd* gene encodes an enzyme that mediates the dissolution of inorganic phosphorus, thereby facilitating the phosphorus cycle in the soil (Liang et al., 2020). The influence of AP and TP on the bacterial community within the restoration areas becomes more pronounced as altitude decreases (Fig. 5). This implies that phosphorus may be a limiting nutrient during soil recovery (Liang et al., 2020; Li et al., 2016; Liu et al., 2023). The mechanism of microbial phosphorus transformation involves phosphate-solubilizing bacteria in the soil secreting organic acids to increase the solubility of inorganic phosphates or organic phosphorus (such as inositol phosphates), converting them into readily available phosphorus within the soil (Yan et al., 2023). This process triggers microbial uptake of available phosphorus, which is then assimilated into their biomass, resulting in intracellular phosphorus compounds, such as nucleic acids and phospholipids (Liang et al., 2020; Luo et al., 2022). As altitude decreases, the diversity and stability of the bacterial community increase (Cui et al., 2019), while the predation of phosphate-solubilizing bacteria on phosphorus intensifies (Alori et al., 2017). This supports the competition hypothesis that limited nutrients suppress microbial diversity through competitive exclusion (Kaspari et al., 2017). Our study indirectly supports these perspectives. We found an increasing correlation and influence of TP on the structure and distribution of bacterial communities (Fig. 5C and F), and microorganisms use various strategies such as enhancing bacterial chemotaxis (Fig. S1), to mitigate phosphorus limitations in the soil. Subsurface soil organic phosphorus and soil pH more effectively regulate the development of microbial communities during soil restoration. The variations in soil nutrient data across the study area also effectively reflect this trend. The surface soil in the densely vegetated A2 and A3 elevation bands exhibits

higher AP content (Table S2), possibly due to the upward migration of AP driven by plant root activity.

In our study, we found a strong correlation between meteorological factors and bacterial communities. Specifically, temperature, relative humidity, and air pressure were identified as having a direct impact on various biological metabolic activities within the soil (Fig. S1). Suitable temperatures are crucial for enzymatic reactions in bacterial metabolism (Chen et al., 2017). The feedback processes between soil moisture and the atmosphere influence both soil moisture content and soil respiration (Humphrey et al., 2021). Sufficient soil moisture and porosity provide essential environmental conditions for the formation of fungal hyphae and the reconstruction of the soil environment (Ciarkowska et al., 2016; Witzgall et al., 2021). Our research also revealed that the content and distribution of soil pH and various phosphorus components are influenced by meteorological factors (Fig. 4). A comprehensive meta-analysis conducted by Li et al. (2022), which included 55 studies from 18 countries and various mining sites, demonstrated that different climate types can influence the succession of soil ecosystems in mining areas. This is likely due to their effects on the content and distribution of soil physicochemical properties. In the study area, the climate exhibits noticeable variations with every 300-m increase in elevation (Table 1). Given its strong correlation with soil nutrients (Fig. 4), we believe that in such ecologically fragile regions, the impact of climate on soil nutrient availability and bacterial community development warrants further investigation.

4.3. Impact of environmental factors on bacterial community stability and assembly

The formation and evolution of bacterial communities play a pivotal role in soil restoration, stabilization, and the proper functioning of essential ecological cycling processes (Kou et al., 2023). Bacterial communities characterized by higher phylogenetic diversity are typically more stable and demonstrate enhanced resistance to disturbances (Xun et al., 2021). The co-occurrence network derived from soil bacteria and microorganisms effectively demonstrates the differential effects of various environmental factors on the stability of bacterial development (Fig. 6A). Our findings contrast with those of Liu et al. (2023), where the microbial networks in the restoration areas were more complex and stable compared to those in undisturbed areas, This may be attributed to the different soil properties of the mining areas we studied. Nevertheless, our results concur with the findings of Wang et al. (2024), indicating that the co-occurrence network of bacteria and soil factors becomes progressively simpler along the restoration gradient, this may reflect the commonality of slope restoration methods. We observed that the co-occurrence networks influenced by pH and phosphorus maintain relative independence and stability across different altitude zones. Both TP and pH synergistically contribute to the stability of the soil ecosystem. Bacteria excrete organic acids to augment the bioavailability of phosphorus in the soil, simultaneously modulating soil pH through feedback mechanisms (Atasoy and Cetecioglu, 2022). Furthermore, fluctuations in environmental pH can alter other metabolic pathways and bacterial reaction rates (Bevilacqua et al., 2021). Within the A2 zone, the microbial network structure, which is controlled by TP and AP, reveals that *Patescibacteria,* despite its low abundance, demonstrates the highest proportion. This observation underscores the correlation between rare bacterial phyla and phosphorus (Gao et al., 2024).

The stability indicators of nodes within the co-occurrence network revealed disparities in the contributions of various soil environmental factors to bacterial community stability (Fig. 6B and Table S4). This finding aligns with the results of the Mantel test (Fig. 4), which showed a stronger correlation in the A1 and A2 zones compared to the A3 zone. Soil nutrients are instrumental in the construction of microbial communities (Jia et al., 2024), the dependence of these communities on nutrients decreases as they stabilize and diversity increases at lower altitudes (Tables 2 and 3). The higher closeness suggests that TP is more central within the network. Our findings indicate a strong correlation between phosphorus and the synthesis of essential amino acids (Fig. S1), suggesting that adequate phosphorus in the soil can enhance microbial diversity (Kaspari et al., 2017). Most organic acids produced by microorganisms have phosphorus-solubilizing functions (Liang et al., 2020), with key phosphate-solubilizing bacteria surrounding phosphate mineral particles to facilitate decomposition, and assemble their communities in these areas (Alori et al., 2017). Given the thin soil layer in the mining area, most of the inorganic phosphate in the soil derives from deep rock minerals (Wang et al., 2024), potentially explaining why TP has a higher closeness in deeper soils. The betweenness of soil factors at the A3R is higher than at A1R and A2R (Fig. S4), suggesting that at lower altitudes, environmental factors exerting a greater influence on the connections act as a "bridge" within bacterial networks. The majority of the shortest paths in the network pass through TP nodes, indicating that phosphorus may facilitate frequent nutrient transfer among different bacteria and limit community development (Yan et al., 2023).

Soil properties play a pivotal role in shaping microbial community assembly, which in turn dictates their functional attributes (Abdu et al., 2017; Pu, 2022; Qiu et al., 2021). Moreover, the assembly of bacterial communities is instrumental in enhancing soil multifunctionality (Jia et al., 2024). Li et al. (2014) assessed the phylogenetic affinity among species within microbial communities across different altitudinal zones in the Hengduan Mountains using the nearest taxon index. Their findings revealed phylogenetic clustering between altitudes of 4300 m and 5500 m. However, above 5500 m, the NTI suggested a randomized phylogenetic structure. Yang et al. (2024) discovered that bacterial communities possessing the mineralization organic phosphorus gene (*phoD*) not only modulate phosphorus levels in the soil but also propel their community assembly. Our research aligns with these findings, as the centrality of TP in the co-occurrence network suggests that bacteria foster community diversity through the mineralization of organic phosphorus (Yan et al., 2023), transitioning from a dispersed to an aggregated developmental state (with NTI values transitioning from negative to positive). The structural equation model corroborates our hypothesis (Fig. 7). The delicate ecosystem of the Tibetan Plateau exhibits pronounced sensitivity to climatic variations across different elevations (Cui et al., 2019). Climatic conditions act as a physical determinant, directly impacting bacterial physiology and metabolism, and subsequently influencing community evolution (Wu et al., 2022). Additionally, they can indirectly affect the intrinsic physiological and biochemical processes in the soil by modifying key physicochemical parameters (such as pH and TP), thereby influencing bacterial biosynthesis, community assembly (NTI), and diversity indices (α and β).

5. Conclusion

In summary, during the restoration of slope soil in alpine metal mining areas, soil pH and TP content emerge as the most influential predictors of bacterial community characteristics. Their spatial dynamics significantly impact bacterial community diversity and assembly mechanisms. As a nutrient-limiting factor, the availability and immobilization of subsurface soil phosphorus accompany the entire course of soil system development. It plays a pivotal role in the cyclical evolution of the microbial community while simultaneously enhancing the soil's physical structure and physicochemical properties. This interaction signifies a co-evolutionary process wherein soil organisms and the soil's physicochemical properties mutually influence each other, driving the soil ecosystem towards increased stability and maturity through ongoing iteration and succession. Despite the challenges posed by the harsh environment of alpine metal mining areas, this study offers fresh research perspectives and theoretical underpinning for understanding the mechanisms behind bacterial community assembly during slope restoration of slopes in such regions. Our study has certain limitations, as it provides only a snapshot of bacterial community structure after three years of soil restoration. Long-term monitoring is required to

capture the complete trajectory of microbial succession and ecosystem recovery. Additionally, fungal community dynamics were not examined in this study. However, considering the crucial role of fungi in soil structure formation, we are currently analyzing fungal communities based on our 2024 sampling data. Future research may integrate metagenomic and transcriptomic approaches to investigate functional genes associated with soil restoration processes (e.g., phosphorus solubilization and pollutant degradation) and the role of plant-microbe-soil feedback in shaping restoration outcomes.

CRediT authorship contribution statement

Huanyu Zhou: Writing – review & editing, Writing – original draft, Visualization, Software, Methodology, Investigation, Data curation. **Xiaotong Liu:** Methodology, Investigation, Data curation. **Xianlei Gao:** Investigation, Formal analysis. **Yan Wang:** Resources, Project administration. **Lanlan Ye:** Software, Methodology. **Junxi Wu:** Writing – review & editing, Supervision, Funding acquisition, Conceptualization. **Mingxue Xiang:** Writing – review & editing, Software, Investigation, Conceptualization.

Declaration of competing interest

The authors declare that they have no known competing financial interests or personal relationships that could have appeared to influence the work reported in this paper.

Acknowledgments

This work is supported by the Science and Technology Program of Lhasa City (LSKJ202318).

Appendix A. Supplementary data

Supplementary data to this article can be found online at https://doi.org/10.1016/j.envres.2025.121432.

Data availability

Data will be made available on request.

References

Abbott, D.e., Essington, M.e., Mullen, M.d., Ammons, J.t., 2001. Fly ash and lime-stabilized biosolid mixtures in mine spoil reclamation: simulated weathering. J. Environ. Qual. 30, 608–616. https://doi.org/10.2134/jeq2001.302608x.

Abdu, N., Abdullahi, A.A., Abdulkadir, A., 2017. Heavy metals and soil microbes. Environ. Chem. Lett. 15, 65–84. https://doi.org/10.1007/s10311-016-0587-x.

Adriano, D.C., Wenzel, W.W., Vangronsveld, J., Bolan, N.S., 2004. Role of assisted natural remediation in environmental cleanup. Geoderma, Biogeochemical processes and the role of heavy metals in the soil environment 122, 121–142. https://doi.org/10.1016/j.geoderma.2004.01.003.

Alori, E.T., Glick, B.R., Babalola, O.O., 2017. Microbial phosphorus solubilization and its potential for use in sustainable agriculture. Front. Microbiol. 8. https://doi.org/10.3389/fmicb.2017.00971.

Altimira, F., Carolina, Yáez, Bravo, G., Myriam, González, Rojas, L.A., Seeger, M., 2012. Characterization of copper-resistant bacteria and bacterial communities from copper-polluted agricultural soils of central Chile. BMC Microbiol. 12. https://doi.org/10.1186/1471-2180-12-193.

Atasoy, M., Cetecioglu, Z., 2022. The effects of pH on the production of volatile fatty acids and microbial dynamics in long-term reactor operation. J. Environ. Manage. 319, 115700. https://doi.org/10.1016/j.jenvman.2022.115700.

Atasoy, M., Eyice, O., Schnürer, A., Cetecioglu, Z., 2019. Volatile fatty acids production via mixed culture fermentation: revealing the link between pH, inoculum type and bacterial composition. Bioresour. Technol. 292, 121889. https://doi.org/10.1016/j.biortech.2019.121889.

Bahram, M., Hildebrand, F., Forslund, S.K., Anderson, J.L., Soudzilovskaia, N.A., Bodegom, P.M., Bengtsson-Palme, J., Anslan, S., Coelho, L.P., Harend, H., Huerta-Cepas, J., Medema, M.H., Maltz, M.R., Mundra, S., Olsson, P.A., Pent, M., Põlme, S., Sunagawa, S., Ryberg, M., Tedersoo, L., Bork, P., 2018. Structure and function of the global topsoil microbiome. Nature 560, 233–237. https://doi.org/10.1038/s41586-018-0386-6.

Banerjee, S., Ghosh, S., Chakraborty, S., Sarkar, D., Datta, R., Bhattacharyya, P., 2024. Synergistic impact of bioavailable PHEs and alkalinity on microbial diversity and traits in agricultural soil adjacent to chromium-asbestos mines. Environ. Pollut. 350, 124021. https://doi.org/10.1016/j.envpol.2024.124021.

Baselga, A., 2012. The relationship between species replacement, dissimilarity derived from nestedness, and nestedness. Glob. Ecol. Biogeogr. 21, 1223–1232. https://doi.org/10.1111/j.1466-8238.2011.00756.x.

Baselga, A., 2010. Partitioning the turnover and nestedness components of beta diversity. Glob. Ecol. Biogeogr. 19, 134–143. https://doi.org/10.1111/j.1466-8238.2009.00490.x.

Baselga, A., Orme, C.D.L., 2012. betapart: an R package for the study of beta diversity. Methods Ecol. Evol. 3, 808–812. https://doi.org/10.1111/j.2041-210X.2012.00224.x.

Bastida, F., Eldridge, D.J., García, C., Kenny Png, G., Bardgett, R.D., Delgado-Baquerizo, M., 2021. Soil microbial diversity–biomass relationships are driven by soil carbon content across global biomes. ISME J. 15, 2081–2091. https://doi.org/10.1038/s41396-021-00906-0.

Beattie, R.E., Henke, W., Campa, M.F., Hazen, T.C., McAliley, L.R., Campbell, J.H., 2018. Variation in microbial community structure correlates with heavy-metal contamination in soils decades after mining ceased. Soil Biol. Biochem. 126, 57–63. https://doi.org/10.1016/j.soilbio.2018.08.011.

Benjamini, Y., Yekutieli, D., 2001. The control of the false discovery rate in multiple testing under dependency. Ann. Stat. 29, 1165–1188. https://doi.org/10.1214/aos/1013699998.

Bevilacqua, R., Regueira, A., Mauricio-Iglesias, M., Lema, J.M., Carballa, M., 2021. Steering the conversion of protein residues to volatile fatty acids by adjusting pH. Bioresour. Technol. 320, 124315. https://doi.org/10.1016/j.biortech.2020.124315.

Bohan, W., Huanyan, L., Xitong, W., Huakang, L., He, P., Mingping, S., Fei, X., Heng, X., 2022. Effects of environmental factors on soil bacterial community structure and diversity in different contaminated districts of Southwest China mine tailings. Sci. Total Environ. 802.

Caporaso, J.G., Lauber, C.L., Walters, W.A., Berg-Lyons, D., Huntley, J., Fierer, N., Owens, S.M., Betley, J., Fraser, L., Bauer, M., Gormley, N., Gilbert, J.A., Smith, G., Knight, R., 2012. Ultra-high-throughput microbial community analysis on the Illumina HiSeq and MiSeq platforms. ISME J. 6, 1621–1624. https://doi.org/10.1038/ismej.2012.8.

Chen, L., Li, J., Chen, Y., Huang, L., Hua, Z., Hu, M., Shu, W., 2013. Shifts in microbial community composition and function in the acidification of a lead/zinc mine tailings. Environ. Microbiol. 15, 2431–2444. https://doi.org/10.1111/1462-2920.12114.

Chen, Y.-L., Deng, Y., Ding, J.-Z., Hu, H.-W., Xu, T.-L., Li, F., Yang, G.-B., Yang, Y.-H., 2017. Distinct microbial communities in the active and permafrost layers on the Tibetan Plateau. Mol. Ecol. 26, 6608–6620. https://doi.org/10.1111/mec.14396.

Ciarkowska, K., Gargiulo, L., Mele, G., 2016. Natural restoration of soils on mine heaps with similar technogenic parent material: a case study of long-term soil evolution in Silesian-Krakow Upland Poland. Geoderma 261, 141–150. https://doi.org/10.1016/j.geoderma.2015.07.018.

Cole, J.R., Wang, Q., Fish, J.A., Chai, B., McGarrell, D.M., Sun, Y., Brown, C.T., Porras-Alfaro, A., Kuske, C.R., Tiedje, J.M., 2014. Ribosomal Database Project: data and tools for high throughput rRNA analysis. Nucleic Acids Res. 42, D633–D642. https://doi.org/10.1093/nar/gkt1244.

Cui, Y., Bing, H., Fang, L., Wu, Y., Yu, J., Shen, G., Jiang, M., Wang, X., Zhang, X., 2019. Diversity patterns of the rhizosphere and bulk soil microbial communities along an altitudinal gradient in an alpine ecosystem of the eastern Tibetan Plateau. Geoderma 338, 118–127. https://doi.org/10.1016/j.geoderma.2018.11.047.

Ding, M., Zhang, Y., Sun, X., Liu, L., Wang, Z., Bai, W., 2013. Spatiotemporal variation in alpine grassland phenology in the Qinghai-Tibetan Plateau from 1999 to 2009. Chin. Sci. Bull. 58, 396–405. https://doi.org/10.1007/s11434-012-5407-5.

Douglas, G.M., Maffei, V.J., Zaneveld, J.R., Yurgel, S.N., Brown, J.R., Taylor, C.M., Huttenhower, C., Langille, M.G.I., 2020. PICRUSt2 for prediction of metagenome functions. Nat. Biotechnol. 38, 685–688. https://doi.org/10.1038/s41587-020-0548-6.

Gao, Y., Liu, S., Liu, Y., Zhang, H., Li, J., 2024. Influences of revegetation type and age on soil C-, N- and P- cycling genes in opencast mining areas on the Loess Plateau. Appl. Soil Ecol. 203, 105649. https://doi.org/10.1016/j.apsoil.2024.105649.

García-Palacios, P., Bowker, M.A., Chapman, S.J., Maestre, F.T., Soliveres, S., Gallardo, A., Valladares, F., Guerrero, C., Escudero, A., 2011. Early-successional vegetation changes after roadside prairie restoration modify processes related with soil functioning by changing microbial functional diversity. Soil Biol. Biochem. 43, 1245–1253. https://doi.org/10.1016/j.soilbio.2011.02.014.

Green, J.L., Bohannan, B.J.M., Whitaker, R.J., 2008. Microbial biogeography: from taxonomy to traits. Science 320, 1039–1043. https://doi.org/10.1126/science.1153475.

Griffiths, R.I., Whiteley, A.S., O'Donnell, A.G., Bailey, M.J., 2000. Rapid method for coextraction of DNA and RNA from natural environments for analysis of ribosomal DNA- and rRNA-based microbial community composition. Appl. Environ. Microbiol. 66, 5488–5491. https://doi.org/10.1128/AEM.66.12.5488-5491.2000.

Gunathunga, S.U., Gagen, E.J., Evans, P.N., Erskine, P.D., Southam, G., 2023. Anthropedogenesis in coal mine overburden; the need for a comprehensive, fundamental biogeochemical approach. Sci. Total Environ. 892, 164515. https://doi.org/10.1016/j.scitotenv.2023.164515.

Hauke, J., Kossowski, T., 2011. Comparison of values of Pearson's and spearman's correlation coefficients on the same sets of data. QUAGEO 30, 87–93. https://doi.org/10.2478/v10117-011-0021-1.

Hou, D., O'Connor, D., Igalavithana, A.D., Alessi, D.S., Luo, J., Tsang, D.C.W., Sparks, D. L., Yamauchi, Y., Rinklebe, J., Ok, Y.S., 2020. Metal contamination and

bioremediation of agricultural soils for food safety and sustainability. Nat. Rev. Earth Environ. 1, 366–381. https://doi.org/10.1038/s43017-020-0061-y.
Hou, Z., Yang, Z., Qu, X., Meng, X., Li, Z., Beaudoin, G., Rui, Z., Gao, Y., Zaw, K., 2009. The Miocene Gangdese porphyry copper belt generated during post-collisional extension in the Tibetan Orogen. Ore Geol. Rev. 36, 25–51. https://doi.org/10.1016/j.oregeorev.2008.09.006.
Hudson-Edwards, K., 2016. Tackling mine wastes. Science 352, 288–290. https://doi.org/10.1126/science.aaf3354.
Humphrey, V., Berg, A., Ciais, P., Gentine, P., Jung, M., Reichstein, M., Seneviratne, S.I., Frankenberg, C., 2021. Soil moisture–atmosphere feedback dominates land carbon uptake variability. Nature 592, 65–69. https://doi.org/10.1038/s41586-021-03325-5.
Janczyk, M., Pfister, R., 2023. One-way analysis of variance (ANOVA). In: Janczyk, M., Pfister, R. (Eds.), Understanding Inferential Statistics: from A for Significance Test to Z for Confidence Interval. Springer, Berlin, Heidelberg, pp. 97–125. https://doi.org/10.1007/978-3-662-66786-6_8.
Jia, J., Hu, G., Ni, G., Xie, M., Li, R., Wang, G., Zhang, J., 2024. Bacteria drive soil multifunctionality while fungi are effective only at low pathogen abundance. Sci. Total Environ. 906, 167596. https://doi.org/10.1016/j.scitotenv.2023.167596.
Jiang, S., Xing, Y., Liu, G., Hu, C., Wang, X., Yan, G., Wang, Q., 2021. Changes in soil bacterial and fungal community composition and functional groups during the succession of boreal forests. Soil Biol. Biochem. 161, 108393. https://doi.org/10.1016/j.soilbio.2021.108393.
Jin, J., Zhao, D., Wang, J., Wang, Y., Zhu, H., Wu, Y., Fang, L., Bing, H., 2024. Fungal community determines soil multifunctionality during vegetation restoration in metallic tailing reservoir. J. Hazard Mater. 478, 135438. https://doi.org/10.1016/j.jhazmat.2024.135438.
Jost, L., 2007. Partitioning diversity into independent alpha and beta components. Ecology 88, 2427–2439. https://doi.org/10.1890/06-1736.1.
Ju, W., Li, J., Yu, W., Zhang, R., 2016. iGraph: an incremental data processing system for dynamic graph. Front. Comput. Sci. 10, 462–476. https://doi.org/10.1007/s11704-016-5485-7.
Kanehisa, M., Goto, S., 2000. KEGG: kyoto encyclopedia of genes and genomes. Nucleic Acids Res. 28, 27–30. https://doi.org/10.1093/nar/28.1.27.
Kaspari, M., Bujan, J., Weiser, M.D., Ning, D., Michaletz, S.T., Zhili, H., Enquist, B.J., Waide, R.B., Zhou, J., Turner, B.L., Wright, S.J., 2017. Biogeochemistry drives diversity in the prokaryotes, fungi, and invertebrates of a Panama forest. Ecology 98, 2019–2028. https://doi.org/10.1002/ecy.1895.
Kenarova, A., Radeva, G., Traykov, I., Boteva, S., 2014. Community level physiological profiles of bacterial communities inhabiting uranium mining impacted sites. Ecotoxicol. Environ. Saf. 100, 226–232. https://doi.org/10.1016/j.ecoenv.2013.11.012.
Kou, B., He, Y., Wang, Y., Qu, C., Tang, J., Wu, Y., Tan, W., Yuan, Y., Yu, T., 2023. The relationships between heavy metals and bacterial communities in a coal gangue site. Environ. Pollut. 322, 121136. https://doi.org/10.1016/j.envpol.2023.121136.
Kuang, J., Huang, L., He, Z., Chen, L., Hua, Z., Jia, P., Li, S., Liu, J., Li, J., Zhou, J., Shu, W., 2016. Predicting taxonomic and functional structure of microbial communities in acid mine drainage. ISME J. 10, 1527–1539. https://doi.org/10.1038/ismej.2015.201.
Lefcheck, J.S., 2016. piecewiseSEM: piecewise structural equation modelling in r for ecology, evolution, and systematics. Methods Ecol. Evol. 7, 573–579. https://doi.org/10.1111/2041-210X.12512.
Legendre, P., Borcard, D., Roberts, D.W., 2012. Variation partitioning involving orthogonal spatial eigenfunction submodels. Ecology 93 (1), 1234–1240. https://doi.org/10.1890/11-2028.
Li, S., Wu, J., Huo, Y., Zhao, X., Xue, L., 2021. Profiling multiple heavy metal contamination and bacterial communities surrounding an iron tailing pond in Northwest China. Sci. Total Environ. 752, 141827. https://doi.org/10.1016/j.scitotenv.2020.141827.
Li, S., Zhang, L., Fang, W., Shen, Z., 2024. Variations in bacterial community succession and assembly mechanisms with mine age across various habitats in coal mining subsidence water areas. Sci. Total Environ. 948, 174822. https://doi.org/10.1016/j.scitotenv.2024.174822.
Li, T., Wang, S., Liu, C., Yu, Y., Zong, M., Duan, C., 2024. Soil microbial communities' contributions to soil ecosystem multifunctionality in the natural restoration of abandoned metal mines. J. Environ. Manage. 353, 120244. https://doi.org/10.1016/j.jenvman.2024.120244.
Li, T., Wu, M., Duan, C., Li, S., Liu, C., 2022. The effect of different restoration approaches on vegetation development in metal mines. Sci. Total Environ. 806, 150626. https://doi.org/10.1016/j.scitotenv.2021.150626.
Li, X.-H., Zhu, X.-X., Niu, Y., Sun, H., 2014. Phylogenetic clustering and overdispersion for alpine plants along elevational gradient in the Hengduan Mountains Region, southwest China. J. Syst. Evol. 52, 280–288. https://doi.org/10.1111/jse.12027.
Li, Y., Niu, S., Yu, G., 2016. Aggravated phosphorus limitation on biomass production under increasing nitrogen loading: a meta-analysis. Glob. Change Biol. 22, 934–943. https://doi.org/10.1111/gcb.13125.
Liang, J.-L., Liu, J., Jia, P., Yang, T., Zeng, Q., Zhang, S., Liao, B., Shu, W., Li, J., 2020. Novel phosphate-solubilizing bacteria enhance soil phosphorus cycling following ecological restoration of land degraded by mining. ISME J. 14, 1600–1613. https://doi.org/10.1038/s41396-020-0632-4.
Ling, N., Wang, T., Kuzyakov, Y., 2022. Rhizosphere bacteriome structure and functions. Nat. Commun. 13, 836. https://doi.org/10.1038/s41467-022-28448-9.
Liu, J., Li, C., Ma, W., Wu, Z., Liu, W., Wu, W., 2023. Exploitation alters microbial community and its co-occurrence patterns in ionic rare earth mining sites. Sci. Total Environ. 898, 165532. https://doi.org/10.1016/j.scitotenv.2023.165532.
Liu, S., Zeng, J., Yu, H., Wang, C., Yang, Y., Wang, J., He, Z., Yan, Q., 2023. Antimony efflux underpins phosphorus cycling and resistance of phosphate-solubilizing bacteria in mining soils. ISME J. 17, 1278–1289. https://doi.org/10.1038/s41396-023-01445-6.
Lu, Z., Wang, H., Wang, Z., Liu, J., Li, Y., Xia, L., Song, S., 2024. Critical steps in the restoration of coal mine soils: microbial-accelerated soil reconstruction. J. Environ. Manage. 368, 122200. https://doi.org/10.1016/j.jenvman.2024.122200.
Luo, R., Kuzyakov, Y., Zhu, B., Qiang, W., Zhang, Y., Pang, X., 2022. Phosphorus addition decreases plant lignin but increases microbial necromass contribution to soil organic carbon in a subalpine forest. Glob. Change Biol. 28, 4194–4210. https://doi.org/10.1111/gcb.16205.
Ma, S., Zhu, W., Wang, W., Li, X., Sheng, Z., 2023. Microbial assemblies with distinct trophic strategies drive changes in soil microbial carbon use efficiency along vegetation primary succession in a glacier retreat area of the southeastern Tibetan Plateau. Sci. Total Environ. 867, 161587. https://doi.org/10.1016/j.scitotenv.2023.161587.
Ma, X., Qu, H., Liao, S., dai, Y., Ji, Y., Li, J., Chao, L., Liu, H., Bao, Y., 2023. Changes in assembly processes and differential responses of soil microbial communities during mining disturbance in mining reclamation and surrounding grassland. Catena 231, 107332. https://doi.org/10.1016/j.catena.2023.107332.
Minchin, P.R., 1987. An evaluation of the relative robustness of techniques for ecological ordination. Vegetatio 69, 89–107. https://doi.org/10.1007/BF00038690.
More, K.S., Wolkersdorfer, C., 2024. The pH paradox. Sci. Total Environ. 946, 174099. https://doi.org/10.1016/j.scitotenv.2024.174099.
Park, I., Tabelin, C.B., Jeon, S., Li, X., Seno, K., Ito, M., Hiroyoshi, N., 2019. A review of recent strategies for acid mine drainage prevention and mine tailings recycling. Chemosphere 219, 588–606. https://doi.org/10.1016/j.chemosphere.2018.11.053.
Pérez Castro, S., Cleland, E.E., Wagner, R., Sawad, R.A., Lipson, D.A., 2019. Soil microbial responses to drought and exotic plants shift carbon metabolism. ISME J. 13, 1776–1787. https://doi.org/10.1038/s41396-019-0389-9.
Pu, Q., 2022. Mercury drives microbial community assembly and ecosystem multifunctionality across a Hg contamination gradient in rice paddies. J. Hazard Mater.
Qiu, L., Zhang, Q., Zhu, H., Reich, P.B., Banerjee, S., van der Heijden, M.G.A., Sadowsky, M.J., Ishii, S., Jia, X., Shao, M., Liu, B., Jiao, H., Li, H., Wei, X., 2021. Erosion reduces soil microbial diversity, network complexity and multifunctionality. ISME J. 15, 2474–2489. https://doi.org/10.1038/s41396-021-00913-1.
Qu, X., 2004. Melt components derived from a subducted slab in late orogenic ore-bearing porphyries in the Gangdese copper belt, southern Tibetan plateau. Lithos 74, 131–148. https://doi.org/10.1016/j.lithos.2004.01.003.
Quinn, G.P., Keough, M.J., 2002. Experimental design and data analysis for biologists. High. Educ. Camb. Univ. Press. https://doi.org/10.1017/CBO9780511806384 [WWW Document].
Santamarina, J.C., Torres-Cruz, L.A., Bachus, R.C., 2019. Why coal ash and tailings dam disasters occur. Science 364, 526–528. https://doi.org/10.1126/science.aax1927.
Shannon, P., Markiel, A., Ozier, O., Baliga, N.S., Wang, J.T., Ramage, D., Amin, N., Schwikowski, B., Ideker, T., 2003. Cytoscape: a software environment for integrated models of biomolecular interaction networks. Genome Res. 13, 2498–2504. https://doi.org/10.1101/gr.1239303.
Soininen, J., Heino, J., Wang, J., 2018. A meta-analysis of nestedness and turnover components of beta diversity across organisms and ecosystems. Glob. Ecol. Biogeogr. 27, 96–109. https://doi.org/10.1111/geb.12660.
Song, J., Shen, Q., Wang, L., Qiu, G., Shi, J., Xu, J., Brookes, P.C., Liu, X., 2018. Effects of Cd, Cu, Zn and their combined action on microbial biomass and bacterial community structure. Environ. Pollut. 243, 510–518. https://doi.org/10.1016/j.envpol.2018.09.011.
Tamura, K., Stecher, G., Kumar, S., 2021. MEGA11: molecular evolutionary genetics analysis version 11. Mol. Biol. Evol. 38, 3022–3027. https://doi.org/10.1093/molbev/msab120.
Tang, J., Zhang, L., Zhang, J., Ren, L., Zhou, Y., Zheng, Y., Luo, L., Yang, Y., Huang, H., Chen, A., 2020. Physicochemical features, metal availability and enzyme activity in heavy metal-polluted soil remediated by biochar and compost. Sci. Total Environ. 701, 134751. https://doi.org/10.1016/j.scitotenv.2019.134751.
Tian, Z., Kang, X., Xu, Y., Zhao, B., Chen, Q., Gu, Y., Xiang, Q., Zhao, K., Zou, L., Ma, M., Penttinen, P., Yu, X., 2024. Bacterial community drives soil organic carbon transformation in vanadium titanium magnetite tailings through remediation using Pongamia pinnata. J. Environ. Manage. 360, 121156. https://doi.org/10.1016/j.jenvman.2024.121156.
Venkateswarlu, K., Nirola, R., Kuppusamy, S., Thavamani, P., Naidu, R., Megharaj, M., 2016. Abandoned metalliferous mines: ecological impacts and potential approaches for reclamation. Rev. Environ. Sci. Biotechnol. 15, 327–354. https://doi.org/10.1007/s11157-016-9398-6.
Wagg, C., Bender, S.F., Widmer, F., van der Heijden, M.G.A., 2014. Soil biodiversity and soil community composition determine ecosystem multifunctionality. https://doi.org/10.1073/pnas.1320054111.
Wang, H., Liu, H., Yang, T., Lv, G., Li, W., Chen, Y., Wu, D., 2023. Mechanisms underlying the succession of plant rhizosphere microbial community structure and function in an alpine open-pit coal mining disturbance zone. J. Environ. Manage. 325, 116571. https://doi.org/10.1016/j.jenvman.2022.116571.
Wang, M., Lin, M., Liu, Q., Li, C., Pang, X., 2024. Fungal, but not bacterial, diversity and network complexity promote network stability during roadside slope restoration. Sci. Total Environ. 922, 171007. https://doi.org/10.1016/j.scitotenv.2024.171007.
Wang, S., Yuan, X., Li, T., Yang, J., Zhao, L., Yuan, D., Guo, Z., Liu, C., Duan, C., 2024. Changes in soil microbe-mediated carbon, nitrogen and phosphorus cycling during spontaneous succession in abandoned Pb Zn mining areas. Sci. Total Environ. 920, 171018. https://doi.org/10.1016/j.scitotenv.2024.171018.

Wickham, H., 2016. In: ggplot2: Elegant Graphics for Data Analysis, second ed. Use R! Springer international publishing, Cham.

Witzgall, K., Vidal, A., Schubert, D.I., Höschen, C., Schweizer, S.A., Buegger, F., Pouteau, V., Chenu, C., Mueller, C.W., 2021. Particulate organic matter as a functional soil component for persistent soil organic carbon. Nat. Commun. 12, 4115. https://doi.org/10.1038/s41467-021-24192-8.

Wu, D., Liu, D., Wang, T., Ding, J., He, Y., Ciais, P., Zhang, G., Piao, S., 2021. Carbon turnover times shape topsoil carbon difference between Tibetan Plateau and Arctic tundra. Sci. Bull. 66, 1698–1704. https://doi.org/10.1016/j.scib.2021.04.019.

Wu, Linwei, Zhang, Y., Guo, X., Ning, D., Zhou, X., Feng, J., Yuan, M.M., Liu, S., Guo, J., Gao, Z., Ma, J., Kuang, J., Jian, S., Han, S., Yang, Z., Ouyang, Y., Fu, Y., Xiao, N., Liu, X., Wu, Liyou, Zhou, A., Yang, Y., Tiedje, J.M., Zhou, J., 2022. Reduction of microbial diversity in grassland soil is driven by long-term climate warming. Nat. Microbiol. 7, 1054–1062. https://doi.org/10.1038/s41564-022-01147-3.

Xu, R., Li, B., Xiao, E., Young, L.Y., Sun, X., Kong, T., Dong, Y., Wang, Q., Yang, Z., Chen, L., Sun, W., 2020. Uncovering microbial responses to sharp geochemical gradients in a terrace contaminated by acid mine drainage. Environ. Pollut. 261, 114226. https://doi.org/10.1016/j.envpol.2020.114226.

Xun, W., Liu, Y., Li, W., Ren, Y., Xiong, W., Xu, Z., Zhang, N., Miao, Y., Shen, Q., Zhang, R., 2021. Specialized metabolic functions of keystone taxa sustain soil microbiome stability. Microbiome 9, 35. https://doi.org/10.1186/s40168-020-00985-9.

Yan, J., Lou, L., Bai, W., Zhang, S., Zhang, N., 2023. Phosphorus deficiency is the main limiting factor for re-vegetation and soil microorganisms in Mu Us Sandy Land. Northwest China. Sci. Total Environ. 900, 165770. https://doi.org/10.1016/j.scitotenv.2023.165770.

Yang, L., Wang, Runze, Shi, J., Wang, Rui, Guo, S., 2024. Nitrogen fertilization management is required for soil phosphorus mobilization by *phoD* community assembly and *pqqC* keystone taxa. Pedosphere. https://doi.org/10.1016/j.pedsph.2024.05.004.

Yang, Z., Hou, Z., White, N.C., Chang, Z., Li, Z., Song, Y., 2009. Geology of the post-collisional porphyry copper–molybdenum deposit at Qulong, Tibet. Ore Geol. Rev.

Yeates, C., Gillings, M., Davison, A., Altavilla, N., Veal, D., 1998. Methods for microbial DNA extraction from soil for PCR amplification. Biol. Proced. Online 1, 40–47. https://doi.org/10.1251/bpo6.

Zhang, M., Yu, X., Jiang, G., Zhou, L., Liu, Z., Li, X., Zhang, T., Wen, J., Xia, L., Liu, X., Yin, H., Meng, D., 2024. Response of bacterial ecological and functional properties to anthropogenic interventions during maturation of mine sand soil. Sci. Total Environ. 938, 173354. https://doi.org/10.1016/j.scitotenv.2024.173354.

Zhang, N., Huang, S., Lei, H., Lei, X., Liu, P., Yan, J., 2022. Changes in soil quality over time focusing on organic acid content in restoration areas following coal mining. Catena 218, 106567. https://doi.org/10.1016/j.catena.2022.106567.

Zuo, Y., Li, Y., Chen, H., Ran, G., Liu, X., 2023. Effects of multi-heavy metal composite pollution on microorganisms around a lead-zinc mine in typical karst areas, southwest China. Ecotoxicol. Environ. Saf. 262, 115190. https://doi.org/10.1016/j.ecoenv.2023.115190.